High Expression of Mammalian Target of Rapamycin Is Associated with Better Outcome for Patients with Early Stage Lung Adenocarcinoma

Valsamo K. Anagnostou,[1] Gerold Bepler,[5] Konstantinos N. Syrigos,[2] Lynn Tanoue,[3] Scott Gettinger,[2] Robert J. Homer,[1] Daniel Boffa,[4] Frank Detterbeck,[4] and David L. Rimm[1]

Abstract

Purpose: Mammalian target of rapamycin (mTOR) is a key kinase downstream of phosphoinositide 3-kinase (PI3K)/AKT predominantly involved in translational control in the presence of nutrients and energy. Despite the well known role of mTOR in carcinogenesis, its prognostic potential in lung cancer has not been investigated. Here, we quantitatively assessed mTOR protein expression in two large data sets to investigate the impact of mTOR expression on patient survival.

Experimental Design: Automated quantitative analysis (AQUA), a fluorescent-based method for analysis of *in situ* protein expression, was used to assess mTOR expression in a training cohort of 167 lung cancer patients. An independent cohort of 235 lung cancer patients (from a second institution) was used for validation.

Results: Tumors expressed mTOR in the cytoplasm in 56% and 50% of the cases in training and validation cohorts, respectively; mTOR expression was not associated with standard clinical or pathologic characteristics. Patients with high mTOR expression had a longer median overall survival compared with the low expressers (52.7 versus 38.5 months; log rank $P = 0.06$), which was more prominent in the adenocarcinoma group (55.7 versus 38.88 months; log rank $P = 0.018$). Multivariate analysis revealed an independent lower risk of death for adenocarcinoma and adenocarcinoma stage IA patients with mTOR-expressing tumors (hazard ratio, 0.48; 95% confidence interval, 0.24-0.98; $P = 0.04$, and hazard ratio, 0.12; 95% confidence interval, 0.03-0.72; $P = 0.019$, respectively).

Conclusions: mTOR expression defines a subgroup of patients with a favorable outcome and may be useful for prognostic stratification of lung adenocarcinoma patients as well as incorporation of mTOR into clinical decisions.

Mammalian target of rapamycin (mTOR) regulates cell growth, acting as a master switch between anabolic and catabolic processes (1, 2). mTOR is a key kinase downstream of phosphoinositide 3-kinase (PI3K)/AKT that regulates the initiation of protein translation in response to intracellular concentrations of amino acids and other essential nutrients (3–5). mTOR consists of two complexes: mTORC1 associated with raptor (regulatory-associated protein of mTOR) and mTORC2 interacting with rictor (rapamycin insensitive companion of mTOR); upon phosphorylation, mTORC1 phosphorylates S6 kinase 1 (S6K1) and eukaryotic initiation factor 4E-binding protein 1 (4EBP1) that increase the translation of a set of mRNAs, thus coupling growth stimuli to cell-cycle progression (6). The less-understood mTORC2 complex directly phosphorylates AKT (7, 8), paradoxically allowing mTOR to be both upstream and downstream of itself (2). More recent studies suggest that mTOR can also regulate the transcription of rRNA and tRNA in yeast and mammalian cells (9, 10). Elements of the PI3K/Akt/mTOR pathway have been shown to be implicated in growth factor receptor (11) as well as oncogenic *Ras* (12, 13) signaling in various cancers, especially in case of phosphatase and tensin homologue (PTEN) loss (14). In genetic syndromes that affect the PTEN or PI3K/Akt/mTOR pathway, the use of mTOR inhibitors has shown the potential to control disease progression as well as antitumor activity (15, 16).

mTOR is an attractive target for biological therapies; mTOR inhibitors not only suppress S6K and 4EBP1 (translational inhibition) but can also block G_1-S transition by increasing cyclin D1 turnover (17, 18) and up-regulating the cyclin-dependent kinase inhibitor p27 (19). Interestingly, mTOR inhibition seems to sensitize tumors to DNA-damaging agents,

Authors' Affiliations: [1]Department of Pathology, [2]Section of Medical Oncology, Department of Internal Medicine, Yale Cancer Center, [3]Section of Pulmonary and Critical Care Medicine, and [4]Department of Surgery, Yale University School of Medicine, New Haven, Connecticut; and [5]Division of Thoracic Oncology, Moffitt Cancer Center, Tampa, Florida

Received 1/15/09; revised 3/20/09; accepted 3/20/09; published OnlineFirst 6/9/09.

Grant support: Thoracic Oncology Group, Yale University School of Medicine, New Haven, CT.

The costs of publication of this article were defrayed in part by the payment of page charges. This article must therefore be hereby marked *advertisement* in accordance with 18 U.S.C. Section 1734 solely to indicate this fact.

Note: Supplementary data for this article are available at Clinical Cancer Research Online (http://clincancerres.aacrjournals.org/).

Requests for reprints: David L Rimm, Department of Pathology, BML 116, Yale University School of Medicine, 310 Cedar Street, P.O. Box 208023, New Haven, CT 06520-8023. Phone: 203-757-4204; Fax: 203-737-5089; E-mail: david.rimm@yale.edu.

©2009 American Association for Cancer Research.

doi:10.1158/1078-0432.CCR-09-0099

Downloaded from clincancerres.aacrjournals.org on September 27, 2020. © 2009 American Association for Cancer Research.

Translational Relevance

This work describes the assessment and validation of mammalian target of rapamycin (mTOR) as a prognostic biomarker in lung cancer. It could be used as a single-marker test in patients with stage I adenocarcinoma to help oncologists educate patients regarding recurrence risk, and assist in the decision regarding adjuvant therapy. Also because mTOR is the target of the drug rapamycin, this work suggests future studies to assess this biomarker as a companion diagnostic test for rapamycin.

such as cisplatin, possibly due to down-regulation of the cell cycle inhibitor p21, which is required for G_1/S cell cycle checkpoint induction and subsequent DNA damage repair (20, 21). Moreover, resistance to human epidermal growth factor receptor–targeted therapies has been partially attributed to increased AKT/mTOR signaling in both breast (22) and lung cancer (23). Despite the promising nature of preclinical data, results of early clinical trials have been disappointing in most tumors except for glioblastoma (24, 25), advanced renal cell carcinoma (26), and mantle cell lymphoma (27). It is possible that this lack of success is a result of treatment of patients who are not specifically selected for mTOR pathway activation because there is no predictive test that identifies mTOR-dependent tumors. Here, we studied the level of expression of mTOR in patients with primary lung adenocarcinoma and assessed its prognostic impact.

Materials and Methods

Cohorts. Formalin-fixed paraffin-embedded primary non–small cell lung cancer (NSCLC) tumors from 167 patients who underwent surgery at Yale University/New Haven Hospital from January 1995 to May 2003 were obtained from the archives of the Pathology Department of Yale University. The Yale University cohort consisted of 85 (51%) men and 82 (49%) women with a median age of 64 y. Data on stage according to tumor-node-metastasis system and differentiation and histologic type according to the WHO classification for NSCLC (28) is shown in Supplementary Table S1. All patients were treatment-naïve prior to tumor resection (or acquisition of surgical biopsies for stage IV patients); average follow-up time was 42.14 ± 2.5 mo (median, 27.66; range, 0.13-182.25). In parallel, we assessed a prospectively collected, independent cohort of 235 NSCLC patients diagnosed from 1991 to 2001, obtained from the H. Lee Moffitt Cancer Center. This cohort consisted of 128 (54.5%) men and 107 (45.5%) women with a median age of 70.5 y. Details on stage, differentiation, and histologic type are shown in Supplementary Table S1. All patients had undergone complete surgical resection for NSCLC and 205 patients received no chemotherapy or radiation prior to resection. Average duration of follow-up in this cohort was 52.34 ± 1.97 mo (median, 42.6; range, 0.8-146.4). The study was approved by the institutional review boards of both centers. Written informed consent was obtained for each case prior to inclusion in the study.

Tissue microarrays. Tissue specimens were prepared in a tissue microarray format: representative tumor areas were obtained from formalin-fixed paraffin-embedded specimens of the primary tumor, and two 0.6-mm cores from each tumor block were arrayed in a recipient block. Formalin-fixed paraffin-embedded cell line pellets were used as controls: HT29, Calu-1, H1299, A549, SW-480, H1666, H1355, A431, HCC2279, H1819, HCC193, and H2126 were purchased from the American Type Culture Collection or donated by other labs. Culture conditions and cell-line tissue microarray construction have been published in detail elsewhere (29).

Western blotting. Equivalent amounts of mTOR (20 μg) were resolved by SDS-PAGE in 3% to 8% tris-acetate gels (150 V for 1 h) and transferred at 30 V for 1 h to polyvinylidene difluoride membrane. Immunoblots were probed with a rabbit monoclonal anti-mTOR antibody (rabbit monoclonal, clone 7C10; Cell Signaling Technology) diluted 1/1,000, followed by an antirabbit horseradish peroxidase–conjugated secondary antibody (Santa Cruz Biotechnology) diluted 1/4,000 and detected using enhanced chemiluminescence (GH Healthcare). β-Tubulin (rabbit polyclonal; Cell Signaling Technology) immunoblotting was used to visualize the total protein loading. One-dimensional Western blots were analyzed and quantified using the ImageJ software.[6] Scores generated were further normalized to the maximum β-tubulin band.

Antibodies and immunohistochemistry. The arrays were deparaffinized with xylene, rehydrated, and antigen-retrieved by pressure cooking for 15 min in citrate buffer (pH = 6). Slides were preincubated with 0.3% bovine serum albumin in 0.1 mol/L TBS (pH = 8) for 30 min at room temperature. Slides were then incubated with a cocktail of the mTOR primary antibody (rabbit monoclonal, clone 7C10; Cell Signaling Technology) diluted 1/1,000 and a mouse monoclonal antihuman cytokeratin antibody (clone AE1/AE3, M3515; Dako) diluted 1:100 in bovine serum albumin/TBS overnight at 4°C. This was followed by a 1-h incubation with Alexa 546-conjugated goat antimouse secondary antibody (A11003; Molecular Probes) diluted 1:100 in rabbit EnVision reagent (K4003, Dako). Cyanine 5 (Cy5) directly conjugated to tyramide (FP1117; Perkin-Elmer) at a 1:50 dilution was used as the fluorescent chromagen for target detection. Prolong mounting medium (ProLong Gold, P36931; Molecular Probes) containing 4′,6-diamidino-2-phenylindole was used to identify tissue nuclei. Serial sections of a smaller specialized NSCLC array (NSCLC control array) were stained aside both cohorts to confirm assay reproducibility. A431 cells were used as positive controls as indicated by the manufacturer. Negative control sections, in which the primary antibody was omitted, were used for each immunostaining run.

Automated quantitative analysis. Automated quantitative analysis (AQUA) allows exact measurement of protein concentration within subcellular compartments, as described in detail elsewhere (30). In brief, a series of high-resolution monochromatic images were captured by the PM-2000 microscope (HistoRx). For each histospot, in- and out-of-focus images were obtained using the signal from the 4′,6-diamidino-2-phenylindole, cytokeratin-Alexa 546 and mTOR-Cy5 channel. mTOR was measured using a channel with emission maxima above 620 nm, in order to minimize tissue autofluorescence. Tumor was distinguished from stromal and nonstromal elements by creating an epithelial tumor "mask" from the cytokeratin signal. This created a binary mask (each pixel being either "on" or "off") on the basis of an intensity threshold set by visual inspection of histospots. The AQUA score of mTOR in each subcellular compartment was calculated by dividing the mTOR compartment pixel intensities by the area of the compartment within which they were measured. AQUA scores were normalized to the exposure time and bit depth at which the images were captured, allowing scores collected at different exposure times to be directly comparable.

Deconvolution microscopy. Three-dimensional images at 60× magnification were acquired with the DeltaVision optical sectioning microscope (Applied Precision Inc.) and subjected to deconvolution by the Soft Worx software (Applied Precision Inc.).

Statistical analysis. Pearson's correlation coefficient (R) was used to assess the correlation between AQUA scores from redundant tumor cores as well as the same cores on serial cuts of the NSCLC control array. An $R^2 > 0.4$ was indicative of good inter- and intra-array reproducibility

[6] http://rsbweb.nih.gov/ij/

Downloaded from clincancerres.aacrjournals.org on September 27, 2020. © 2009 American Association for Cancer Research.

and thus the average values for mTOR AQUA scores from duplicate samples were calculated and treated as independent continuous variables. The association between mTOR AQUA scores and other variables was analyzed using Spearman rank test. X-tile software (31) was used to select the optimal mTOR concentration cut point for the Yale University cohort (training set); this cut point was subsequently validated in the Moffitt Cancer Center cohort (validation set). Survival curves for the validation set were constructed using the Kaplan-Meier method, and survival differences were analyzed by the log rank test. Cox proportional hazards regression analysis was used to determine which independent factors jointly had a significant impact on overall survival. All P values were based on two-sided testing and differences were considered significant at $P < 0.05$. All statistical analyses were done using the SPSS software program (version 13.0 for Windows, SPSS Inc.).

Results

Identification of the optimal classification on the basis of mTOR expression (training cohort). In order to assess mTOR expression in a rigorous and reproducible way, total mTOR levels were independently detected by AQUA analysis (Fig. 1A and B) and Western blot (Fig. 1C and D) in cell line controls. Bands on Western blot analysis were quantified and normalized to the β-tubulin control, resulting in a score for relative mTOR expression. The H1299, A431, HT29, H1666, H1355, and HCC193 cell lines showed the same range of mTOR expression on both AQUA and Western blot analysis, and comparison of AQUA and Western blot scores showed an excellent correlation (Pearson's $R = 0.9$; $P < 0.0001$). Evaluation of the inter-array reproducibility did not reveal significant differences between serial sections of the NSCLC control array (Pearson's $R = 0.94$; $P < 0.0001$; Fig. 2A).

mTOR was predominantly expressed in the cytoplasm of NSCLC cell lines (Fig. 1B) as well as NSCLC tumor cells (Fig. 3). A more careful inspection using convolution/deconvolution microscopy revealed a punctate cytoplasmic and perinuclear distribution of mTOR consistent with its known localization to endoplasmic reticulum and Golgi apparatus (Fig. 3D). To assess intratumoral heterogeneity for mTOR expression, we compared AQUA scores from redundant tumor cores and observed significant correlation (Pearson's $R = 0.67$; $P < 0.0001$; Fig. 2B). Therefore, AQUA scores in the cytoplasmic compartment were averaged between redundant histospots, and final scores ranged from 3.2 to 109.5 (mean 32 ± 1.24; median 28.7). Specimens with <5% tumor area per spot were not included in automated quantitative analysis for not being representative of the corresponding tumor specimen.

The potential correlation between mTOR expression and patient characteristics was assessed for patients of the Yale University cohort, and clinicopathologic parameters analyzed included age, gender, histologic type, tumor differentiation, and stage; however, mTOR expression was independent of all parameters studied (Table 1).

We applied X-tile (31) in order to determine the optimal cut point of continuous mTOR AQUA scores; this statistical method assesses every division of continuous variables into ordinal classes and does standard Monte Carlo simulations to

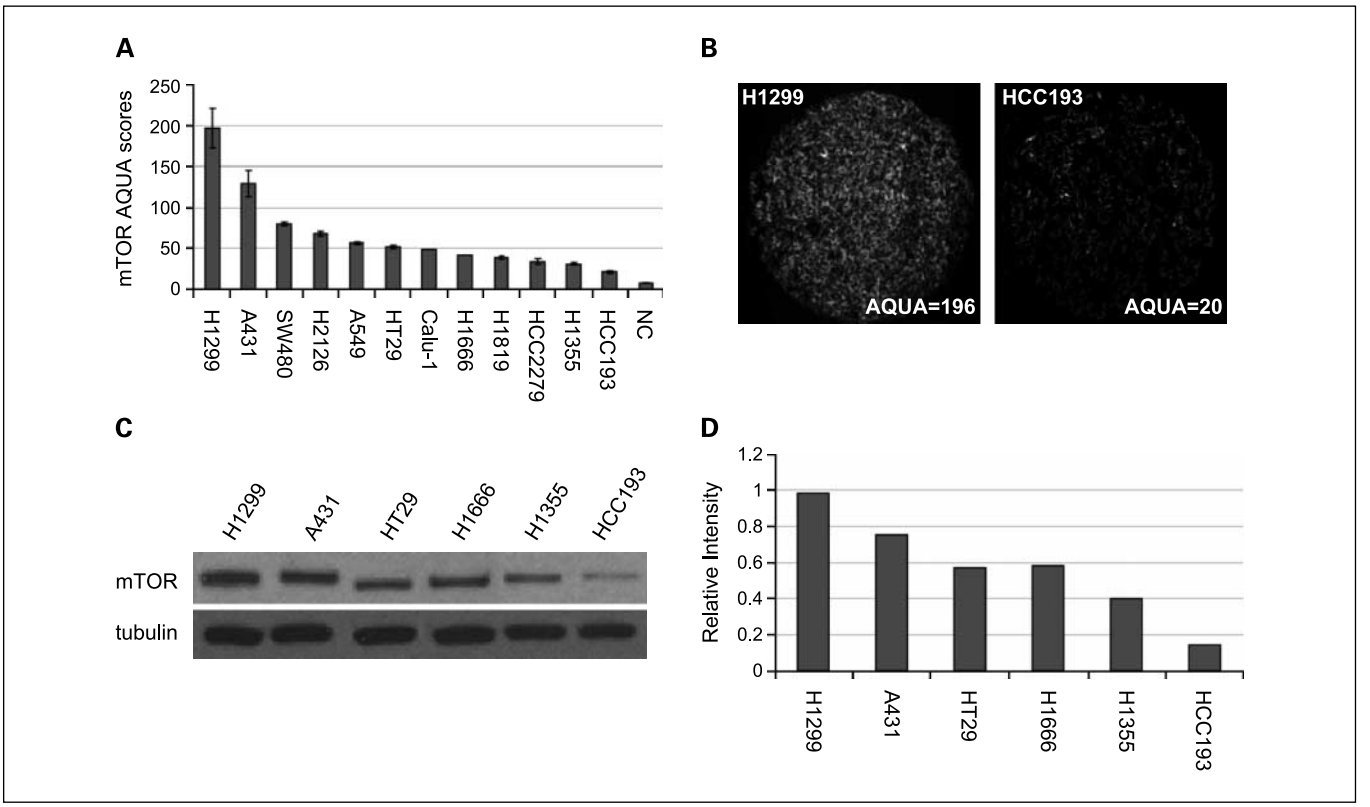

Fig. 1. Distribution of mTOR AQUA scores in cell line controls. *A,* distribution of mTOR AQUA scores in 12 cell line controls embedded in the NSCLC control array; the AQUA score of the negative control (NC) was used as a zero point. *B,* representative immunofluorescence staining in the highest (H1299) and lowest (HCC193) mTOR-expressing lung cancer cell lines. Insets, AQUA scores. *C,* mTOR protein detected by Western blot in the same cell lines; β-tubulin was used as a control. *D,* quantification of mTOR bands on Western blot; the dynamic range of mTOR expression is consistent with AQUA analysis.

Downloaded from clincancerres.aacrjournals.org on September 27, 2020. © 2009 American Association for Cancer Research.

produce χ^2 values that can be maximized to find the optimal cut point in continuous data. Because it is not statistically valid to test multiple divisions with corrections for multiple sampling, rigorous statistical evaluation is achieved by defining divisions in a training set and then validating them in an independent nonoverlapping validation set. On that basis we used the Yale University cohort as a training set to generate a cut point that provides the optimal separation in terms of survival; an AQUA score of 28 was thus selected as the optimal cut point and classified 73 (44%) as low expressers and 94 (56%) of the patients as high expressers; as for adenocarcinoma and stage I adenocarcinoma patients, 60 (60%) and 25 (56%) were stratified in the high group, respectively. Adenocarcinoma patients classified as high mTOR expressers had a better prognosis compared with the low-expressing group (median survival, 27.4 versus 26 months; Fig. 4A), and the same trend was observed in the stage I adenocarcinoma group (median survival, 45.8 versus 44 months; Fig. 4B).

Validation of cut point selection (validation cohort). The cut point generated from the training set was applied in the Moffitt Cancer Center cohort (validation set) in which mTOR expression was assessed in 116 (50%) NSCLC cases: 47 (52%) adenocarcinomas, 38 (48%) squamous cell carcinomas, 13 (59%) bronchioloalveolar carcinomas, 14 (58%) large cell carcinomas, and 4 (100%) neuroendocrine carcinomas. In the stage I adenocarcinoma group 41 (51%) patients were classified as high versus 40 (49%) low expressers. As in the training set mTOR expression was not significantly associated with any clinicopathologic characteristic (Table 1). mTOR AQUA scores for specimens on the validation cohort were converted according to the cell line standard curve (y = 0.84x + 0.52; Fig. 2A), in order to normalize for run-to-run variability.

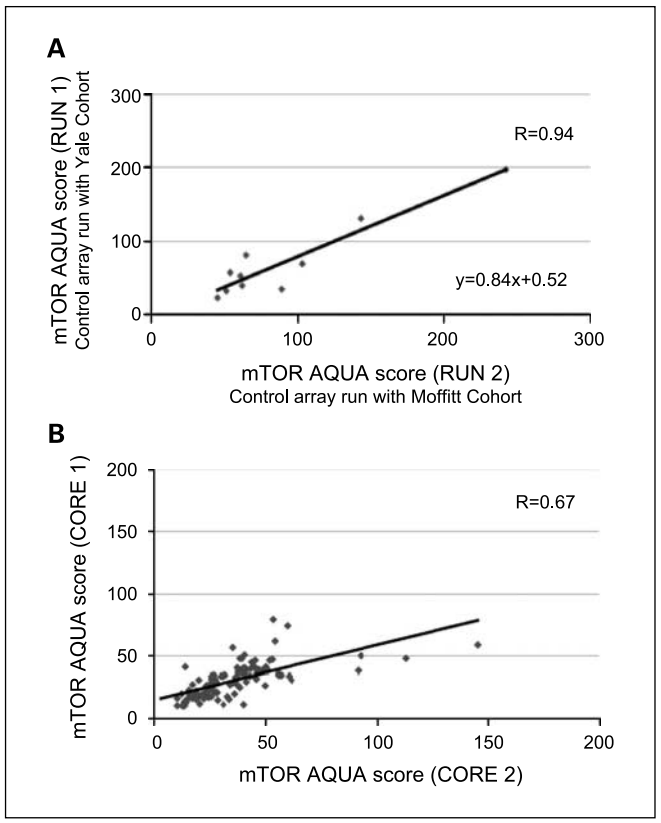

Fig. 2. Assay reproducibility and tumor heterogeneity for mTOR in the training cohort. *A,* plotting AQUA scores of the same cell lines on serial cuts of the NSCLC control array stained aside the two cohorts at different runs provided a standard curve in order to normalize for minimal run to run variability (Pearson's $R = 0.94$ between runs; $P < 0.0001$). *B,* linear regression between mTOR AQUA scores of redundant tumor cores reveals significant correlation (Pearson's $R = 0.67$; $P < 0.0001$).

We then assessed the potential of mTOR to predict survival; among all patients, tumors with high mTOR expression (n = 116) had a higher median survival compared with the low mTOR expressers (n = 105; median survival, 52.7 versus 38.5 months, respectively; log rank P = 0.06). Adenocarcinoma patients with high mTOR expression (n = 47) showed longer survival (median survival 55.7 versus 38.88 months for the high and low group, respectively; log rank P = 0.018; Fig. 4C), and this was also observed in the high mTOR-expressing stage I adenocarcinoma group (n = 41; median survival 54.4 months versus 38 months for the low expressers; log rank P = 0.02; Fig. 4D). Cox univariate analysis with continuous mTOR scores binarized by the optimal cut point revealed that high mTOR expression resulted in 57% to 88% reduction in risk especially for stage IA adenocarcinoma patients [hazards ratio (HR), 0.43; 95% confidence interval (95% CI), 0.21-0.89; P = 0.02 for all patients; HR, 0.44; 95% CI, 0.22-0.88; P = 0.02 for adenocarcinomas; HR, 0.43; 95% CI, 0.21-0.89; P = 0.02 for stage I adenocarcinomas; and HR, 0.12; 95% CI, 0.02-0.55; P = 0.007 for stage IA adenocarcinomas]. Age and tumor size were analyzed as continuous and stage and gender as categorical variables.

Assessment of the independent potential of mTOR to predict survival. Multivariate Cox proportional hazards regression analysis was done to derive risk estimates related to survival for all clinicopathologic characteristics and mTOR expression; cases with missing values were excluded from analysis (Table 2). Age, stage, and mTOR expression were significantly associated with survival for adenocarcinoma patients and mTOR expression retained its prognostic value such that adenocarcinoma patients with high mTOR expression had a 52% reduction in risk (HR, 0.48; 95% CI, 0.24-0.98; P = 0.04). In a subgroup analysis of adenocarcinoma patients with stage I disease, high mTOR expression contributed to the prognostic value of the model (HR, 0.5; 95% CI, 0.24-1; P = 0.06) and the independent favorable prognostic value of mTOR was more prominent for stage IA adenocarcinoma patients (HR, 0.12; 95% CI, 0.03-0.72; P = 0.019; Table 2).

Discussion

Despite promising preclinical data, phase I/II trials have shown that rapamycin and analogues have a limited efficacy as single agents in NSCLC (32, 33). This may be due to the absence of patient selection; therefore, efforts have been made to identify surrogate markers for sensitivity to mTOR inhibition (34). For example, pretreatment and posttreatment tumor profiling showed that resistance to the rapamycin analogue CCI-779 was associated with low baseline AKT and pS6K levels in glioblastomas (25, 35), whereas PTEN loss or AKT activation and pS6K/4EBP1 up-regulation were associated with objective responses in renal cell carcinomas (36, 37). However, no biomarker has been associated with prediction of response in lung cancer, and the molecular phenotype of NSCLC tumors susceptible to mTOR inhibition remains to be defined. The goal

Downloaded from clincancerres.aacrjournals.org on September 27, 2020. © 2009 American Association for Cancer Research.

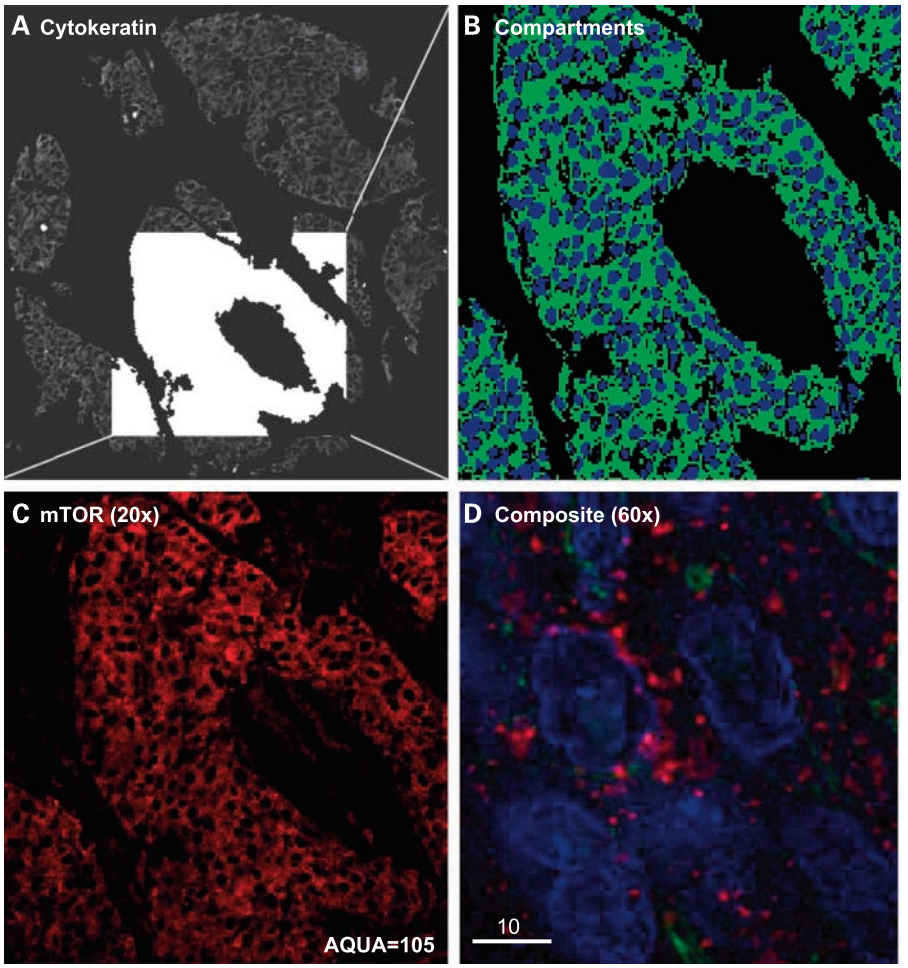

Fig. 3. AQUA of mTOR in lung cancer. *A* to *D,* tumor histospot corresponding to a NSCLC patient with mTOR AQUA score of 105. *A,* cytokeratin-Cy3 image used to identify tumor; inset, the epithelial tumor "mask." *B,* colocalization of subcellular compartments; the nonnuclear (*green*) and nuclear (*blue*) compartment are defined by the cytokeratin and the 4′,6-diamidino-2-phenylindole signal respectively. *C*, mTOR-Cy5 image showing representative cytoplasmic pattern; AQUA score is inset into the bottom right corner. *D,* deconvoluted three-dimensional image acquired by the DeltaVision confocal microscope of the tumor field shown in (*A*) showing multiplex immunostaining with cytokeratin (*green*), 4′,6-diamidino-2-phenylindole (*blue*), and mTOR (*red*); mTOR is predominantly distributed in the cytoplasm and perinuclear area. Original magnification, *A* to *C* ×20; *D* × 60.

of this work was to quantitatively assess mTOR expression and to determine its prognostic value as a preliminary study toward assessment of its predictive value. Because no mutations for the *FRAP* gene have been reported to date, protein levels might serve as a surrogate marker for response to mTOR-targeted agents.

To accurately predict response to mTOR inhibitor therapies, preclinical studies have used phospho p70S6K, phospho 4EBP1, and pAKT (34, 36, 38). This is less accurate in human tumors because the extent of phosphorylation in formalin-fixed paraffin-embedded tissue is often affected by time to fixation and thus can be inaccurate (39). However, we and others have found that the loss of phosphorylation is variable, depending on the site being assessed; in two unpublished studies phospho-p70S6K seems to correlate with the level of the total mTOR protein expression, suggesting that this site may be stable to variations in fixation time. We have no experience with phospho-mTOR, but it has been shown by Balsara and colleagues that high phospho mTOR levels have been detected in 72% of NSCLC (40). This is consistent with our findings in which 56% of the patients were classified as high expressers.

We were unable to find any previous studies assessing the prognostic value of mTOR protein expression in NSCLC. This

Table 1. Correlations between mTOR expression and clinicopathologic factors

Correlations	Stage	Age	Gender	Hist. Type
mTOR levels				
Training cohort	0.06 (NS)	-0.68* (NS)	-0.02 (NS)	-0.05 (NS)
Validation cohort	-0.13 (**$P = 0.05$**)	-0.09* (NS)	-0.09 (NS)	-0.05 (NS)

NOTE: Nonparametric correlations between continuous mTOR AQUA scores and ordinal variables (stage, gender, and histologic type) were assessed with Spearman's rank test.
Statistically significant *P* values ($P < 0.05$) are in boldface.
Abbreviation: NS, nonsignificant.
*Pearson's *R* coefficient was used for parametric correlations with continuous variables (age).

Downloaded from clincancerres.aacrjournals.org on September 27, 2020. © 2009 American Association for Cancer Research.

may be due to the subtlety of the assessment of the cut point. Highly accurate and reproducible measurement of mTOR has been difficult because conventional immunohistochemistry methods have been qualitative and generally not uniformly standardized. To measure proteins in a manner as rigorous as the methods used for genetic signatures, and in order to standardize markers to each other and allow application of rigorous mathematical models, a quantitative approach such as AQUA allowed us to discover this relationship. In fact, it may be difficult or impossible to distinguish positive from negative mTOR based on a conventional optical microscope. In the future, however, it is likely that the subjective and relatively insensitive current immunohistochemistry methods will be replaced by quantitative and reproducible approaches. Although we have used the AQUA method here, other quantitative approaches might equally be used, and allow practical application of these findings in the clinic.

In light of experimental data suggesting mTOR inhibition may slow cancer progression (41) one would expect that high mTOR expression would confer to a worse prognosis, rather than a prolonged survival. One possible explanation is that the activity of mTOR may be controlled at posttranslational levels (42), therefore increased expression does not necessarily equate to cell cycle progression. Moreover, experimental studies have shown that the mTOR pathway regulates cell growth at the expense of proliferation (43) and that a block in the machinery that drives cell cycle progression leads to an increase in cell size (44, 45), thus uncoupling cell growth from cell cycle. Clearly

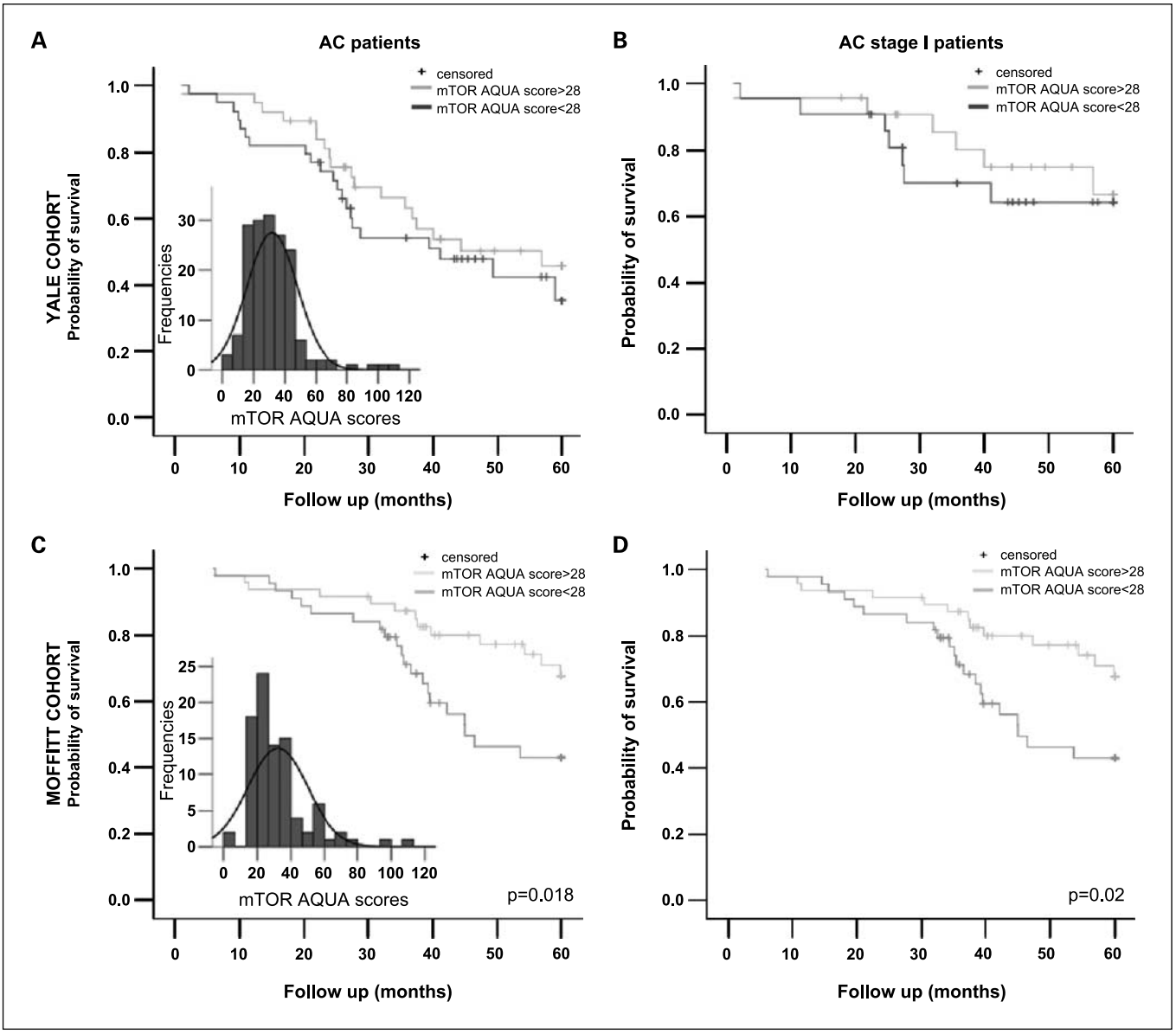

Fig. 4. Disease outcome by mTOR expression in primary lung adenocarcinomas. *A* and *B,* survival curves based on cohort division by the optimal cut point generated from the Yale University Cohort (training set); adenocarcinoma and adenocarcinoma stage I patients classified as high mTOR expressers ($n = 60$ and $n = 25$, respectively) show a benefit towards survival. Inset, distribution of mTOR AQUA scores. *C,* Kaplan-Meier graphical analysis of 5-year survival in adenocarcinoma patients of the Moffitt Cancer Center Cohort (validation set, $n = 97$). Patients with a high mTOR score ($n = 47$) had a significantly higher median survival compared with the low mTOR group (log rank $P = 0.018$). Inset, distribution of mTOR AQUA scores. *D,* Kaplan-Meier survival curves for stage I adenocarcinoma patients of the Moffitt Cancer Center cohort ($n = 87$) classified as high ($n = 41$) versus low mTOR expressers showed a benefit towards survival for the high-expressing group (log rank $P = 0.02$). AC, adenocarcinoma.

Downloaded from clincancerres.aacrjournals.org on September 27, 2020. © 2009 American Association for Cancer Research.

Table 2. Multivariate analysis of overall survival for mTOR expression in lung adenocarcinoma patients

Characteristic	AC patients (n = 97)		AC stage I patients (n = 87)		AC stage IA patients (n = 42)	
	HR (95% CI)	P*	HR (95% CI)	P*	HR (95% CI)	P*
Age	1.04 (0.99-1.08)	*0.07*	1.06 (1.01-1.1)	**0.012**	1.03 (0.94-1.1)	0.5
Gender						
Female	1		1		1	
Male	1.5 (0.76-3.3)	0.21	1.9 (0.89-4.1)	0.1	1.4 (0.33-6.15)	0.6
Size	1. (0. 79-1.25)	0.9	1.01 (0.8-1.26)	0.8	1.15 (0.4-.3.3)	0.8
Stage						
Stage I						
IA	1		1			
IB	2.78 (1.26-6.09)	**0.01**	2.86 (1.3-6.3)	**0.009**		
Stage II	-†					
Stage III	-†					
Stage IV	0.85 (0.19-3.9)	0.8				
mTOR						
Low	1		1		1	
High	0.48 (0.24-0.98)	**0.04**	0.5 (0.24-1)	*0.06*	0.14 (0.03-0.73)	**0.019**

Abbreviation: AC, adenocarcinoma.
*P is given for Cox multivariate analysis. Statistically significant P values ($P < 0.05$) are in boldface, whereas trending P values are in italics.
†HRs could not be estimated for stage II and III due to small number of observations; HR for stage IV patients is estimated based on four observations and is driven by the wide 95% CI.

the functions of mTOR are more complex than just translational control, and crosstalk between pathways could alter its oncogenic potential in NSCLC.

Although we are optimistic that the prognostic findings presented here are likely to portend predictive results, we were unable to obtain information on patients' postoperative treatment or progression-free survival, and the absence of that data represents a limitation of this first report. We have sought mTOR inhibitor trials that would have uniform treatment, but have been unable to obtain tissue. Other limitations include the retrospective nature of the collection of the training cohort; a prognostic trial of a single marker such as this can rarely be prospectively achieved because the cost and effort of prospective trials nearly always mandate a testing of a new therapy. Importantly, the two cohorts are not well matched in terms of disease stage; therefore, we did a separate analysis using stage I adenocarcinoma patients of the Yale University cohort as the training group and validated the cut point generated (an mTOR AQUA score of 27.6) on stage I adenocarcinomas of the Moffitt Cancer Center cohort. This new prognostic stratification reproduced the results analyzed above and all but two patients were classified in the same groups according to mTOR expression. These findings showed that the cut point generated by X-tile analysis of the whole training cohort was robust enough for analysis of the early-stage validation cohort. Although it can be argued that for continuous measurements, no cut point should be defined, the treatment of a patient is a binary decision. Thus, we used a common approach to determine the optimal cut point where we use a training set to find a cut point, then validate it in a completely independent population. Here, we used X-tile as a tool to optimally select a cut point using the Yale cohort (31). Then we validated the cut point in the Moffitt cohort.

In summary, we assessed the prognostic potential of mTOR in NSCLC patients and report that mTOR protein levels are an independent favorable prognostic factor for primary lung adenocarcinoma, especially stage I patients. This observation raises the possibility that total mTOR levels may also have predictive value in a manner analogous to estrogen receptor in breast cancer, identifying a subgroup of patients with better prognosis and serving as a viable target at the same time. Future studies are under way to assess the effect of total protein levels in preclinical models toward the goal of testing mTOR as a companion diagnostic in future clinical trials of mTOR inhibitors.

Disclosure of Potential Conflicts of Interest

D. Rimm, consultant and ownership interest, HistoRx.

Acknowledgments

We thank Dr Seema Agarwal for technical assistance and helpful discussions, and Dr Michael Peyton (UT Southwestern Medical Center, Dallas, TX) for donation of NSCLC cell lines.

References

1. Sarbassov DD, Ali SM, Sabatini DM. Growing roles for the mTOR pathway. Curr Opin Cell Biol 2005;17:596–603.
2. Sabatini DM. mTOR and cancer: insights into a complex relationship. Nat Rev Cancer 2006;6:729–34.
3. Schmelzle T, Hall MN. TOR, a central controller of cell growth. Cell 2000;103:253–62.
4. Thomas G, Hall MN. TOR signalling and control of cell growth. Current opinion in cell biology 1997;9:782–7.
5. Faivre S, Kroemer G, Raymond E. Current development of mTOR inhibitors as anticancer agents. Nat Rev Drug Discov 2006;5:671–88.
6. Hay N, Sonenberg N. Upstream and downstream of mTOR. Genes Dev 2004;18:1926–45.
7. Hresko RC, Mueckler M. mTOR.RICTOR is the Ser473 kinase for Akt/protein kinase B in 3T3–1 adipocytes. The Journal of biological chemistry 2005;280:40406–16.
8. Sarbassov DD, Guertin DA, Ali SM, Sabatini DM. Phosphorylation and regulation of Akt/PKB by the rictor-mTOR complex. Science 2005;307:1098–101.
9. Mahajan PB. Modulation of transcription of rRNA genes by rapamycin. International journal of immunopharmacology 1994;16:711–21.

Downloaded from clincancerres.aacrjournals.org on September 27, 2020. © 2009 American Association for Cancer Research.

10. Leicht M, Simm A, Bertsch G, Hoppe J. Okadaic acid induces cellular hypertrophy in AKR-2B fibroblasts: involvement of the p70S6 kinase in the onset of protein and rRNA synthesis. Cell Growth Differ 1996;7:1199–209.

11. Lee AV, Yee D. Insulin-like growth factors and breast cancer. Biomed Pharmacother 1995;49:415–21.

12. Shaw RJ, Cantley LC. Ras, PI(3)K and mTOR signalling controls tumour cell growth. Nature 2006;441:424–30.

13. Hu Q, Klippel A, Muslin AJ, Fantl WJ, Williams LT. Ras-dependent induction of cellular responses by constitutively active phosphatidylinositol-3 kinase. Science 1995;268:100–2.

14. Neshat MS, Mellinghoff IK, Tran C, et al. Enhanced sensitivity of PTEN-deficient tumors to inhibition of FRAP/mTOR. Proc Natl Acad Sci U S A 2001;98:10314–9.

15. Inoki K, Li Y, Zhu T, Wu J, Guan KL. TSC2 is phosphorylated and inhibited by Akt and suppresses mTOR signalling. Nat Cell Biol 2002;4:648–57.

16. Lee L, Sudentas P, Donohue B, et al. Efficacy of a rapamycin analog (CCI-779) and IFN-γ in tuberous sclerosis mouse models. Genes Chromosomes Cancer 2005;42:213–27.

17. Hashemolhosseini S, Nagamine Y, Morley SJ, Desrivieres S, Mercep L, Ferrari S. Rapamycin inhibition of the G1 to S transition is mediated by effects on cyclin D1 mRNA and protein stability. J Biologic Chem 1998;273:14424–9.

18. Grewe M, Gansauge F, Schmid RM, Adler G, Seufferlein T. Regulation of cell growth and cyclin D1 expression by the constitutively active FRAP-p70s6K pathway in human pancreatic cancer cells. Cancer Res 1999;59:3581–7.

19. Nourse J, Firpo E, Flanagan WM, et al. Interleukin-2-mediated elimination of the p27Kip1 cyclin-dependent kinase inhibitor prevented by rapamycin. Nature 1994;372:570–3.

20. Aoki K, Ogawa T, Ito Y, Nakashima S. Cisplatin activates survival signals in UM-SCC-23 squamous cell carcinoma and these signal pathways are amplified in cisplatin-resistant squamous cell carcinoma. Oncol Rep 2004;11:375–9.

21. Beuvink I, Boulay A, Fumagalli S, et al. The mTOR inhibitor RAD001 sensitizes tumor cells to DNA-damaged induced apoptosis through inhibition of p21 translation. Cell 2005;120:747–59.

22. Nagata Y, Lan KH, Zhou X, et al. PTEN activation contributes to tumor inhibition by trastuzumab, and loss of PTEN predicts trastuzumab resistance in patients. Cancer Cell 2004;6:117–27.

23. Kokubo Y, Gemma A, Noro R, et al. Reduction of PTEN protein and loss of epidermal growth factor receptor gene mutation in lung cancer with natural resistance to gefitinib (IRESSA). Brit J Cancer 2005;92:1711–9.

24. Chang SM, Wen P, Cloughesy T, et al. Phase II study of CCI-779 in patients with recurrent glioblastoma multiforme. Invest New Drugs 2005;23:357–61.

25. Galanis E, Buckner JC, Maurer MJ, et al. Phase II trial of temsirolimus (CCI-779) in recurrent glioblastoma multiforme: a North Central Cancer Treatment Group Study. J Clin Oncol 2005;23:5294–304.

26. Atkins MB, Hidalgo M, Stadler WM, et al. Randomized phase II study of multiple dose levels of CCI-779, a novel mammalian target of rapamycin kinase inhibitor, in patients with advanced refractory renal cell carcinoma. J Clin Oncol 2004;22:909–18.

27. Witzig TE, Geyer SM, Ghobrial I, et al. Phase II trial of single-agent temsirolimus (CCI-779) for relapsed mantle cell lymphoma. J Clin Oncol 2005;23:5347–56.

28. Travis WD BE, Muller-Hermelink HK, Harris CC. WHO classification of tumors of the lung, pleura and mediastinum. Lyon: IARC Press; 2004.

29. McCabe A, Dolled-Filhart M, Camp RL, Rimm DL. Automated quantitative analysis (AQUA) of *in situ* protein expression, antibody concentration, and prognosis. J Natl Cancer Inst 2005;97:1808–15.

30. Camp RL, Chung GG, Rimm DL. Automated subcellular localization and quantification of protein expression in tissue microarrays. Nat Med 2002;8:1323–7.

31. Camp RL, Dolled-Filhart M, Rimm DL. X-tile: a new bio-informatics tool for biomarker assessment and outcome-based cut-point optimization. Clin Cancer Res 2004;10:7252–9.

32. Vignot S, Faivre S, Aguirre D, Raymond E. mTOR-targeted therapy of cancer with rapamycin derivatives. Ann Oncol 2005;16:525–37.

33. Hidalgo M, Buckner JC, Erlichman C, et al. A phase I and pharmacokinetic study of temsirolimus (CCI-779) administered intravenously daily for 5 days every 2 weeks to patients with advanced cancer. Clin Cancer Res 2006;12:5755–63.

34. Boulay A, Zumstein-Mecker S, Stephan C, et al. Antitumor efficacy of intermittent treatment schedules with the rapamycin derivative RAD001 correlates with prolonged inactivation of ribosomal protein S6 kinase 1 in peripheral blood mononuclear cells. Cancer Res 2004;64:252–61.

35. Duran I, Kortmansky J, Singh D, et al. A phase II clinical and pharmacodynamic study of temsirolimus in advanced neuroendocrine carcinomas. Brit J Cancer 2006;95:1148–54.

36. Cho D, Signoretti S, Dabora S, et al. Potential histologic and molecular predictors of response to temsirolimus in patients with advanced renal cell carcinoma. Clin Genitour Cancer 2007;5:379–85.

37. Cho D, Signoretti S, Regan M, Mier JW, Atkins MB. The role of mammalian target of rapamycin inhibitors in the treatment of advanced renal cancer. Clin Cancer Res 2007;13:758–63s.

38. Mabuchi S, Altomare DA, Cheung M, et al. RAD001 inhibits human ovarian cancer cell proliferation, enhances cisplatin-induced apoptosis, and prolongs survival in an ovarian cancer model. Clin Cancer Res 2007;13:4261–70.

39. Baker AF, Dragovich T, Ihle NT, Williams R, Fenoglio-Preiser C, Powis G. Stability of phosphoprotein as a biological marker of tumor signaling. Clin Cancer Res 2005;11:4338–40.

40. Balsara BR, Pei J, Mitsuuchi Y, et al. Frequent activation of AKT in non-small cell lung carcinomas and preneoplastic bronchial lesions. Carcinogenesis 2004;25:2053–9.

41. Boffa DJ, Luan F, Thomas D, et al. Rapamycin inhibits the growth and metastatic progression of non-small cell lung cancer. Clin Cancer Res 2004;10:293–300.

42. Gingras AC, Raught B, Sonenberg N. Regulation of translation initiation by FRAP/mTOR. Genes Dev 2001;15:807–26.

43. Montagne J, Stewart MJ, Stocker H, Hafen E, Kozma SC, Thomas G. Drosophila S6 kinase: a regulator of cell size. Science 1999;285:2126–9.

44. Fingar DC, Salama S, Tsou C, Harlow E, Blenis J. Mammalian cell size is controlled by mTOR and its downstream targets S6K1 and 4EBP1/eIF4E. Genes Dev 2002;16:1472–87.

45. Neufeld TP, de la Cruz AF, Johnston LA, Edgar BA. Coordination of growth and cell division in the Drosophila wing. Cell 1998;93:1183–93.

Downloaded from clincancerres.aacrjournals.org on September 27, 2020. © 2009 American Association for Cancer Research.

AACR American Association for Cancer Research

Clinical Cancer Research

High Expression of Mammalian Target of Rapamycin Is Associated with Better Outcome for Patients with Early Stage Lung Adenocarcinoma

Valsamo K. Anagnostou, Gerold Bepler, Konstantinos N. Syrigos, et al.

Clin Cancer Res 2009;15:4157-4164.

Updated version	Access the most recent version of this article at: http://clincancerres.aacrjournals.org/content/15/12/4157
Supplementary Material	Access the most recent supplemental material at: http://clincancerres.aacrjournals.org/content/suppl/2009/06/15/1078-0432.CCR-09-0099.DC1

Cited articles	This article cites 44 articles, 20 of which you can access for free at: http://clincancerres.aacrjournals.org/content/15/12/4157.full#ref-list-1
Citing articles	This article has been cited by 3 HighWire-hosted articles. Access the articles at: http://clincancerres.aacrjournals.org/content/15/12/4157.full#related-urls

E-mail alerts	Sign up to receive free email-alerts related to this article or journal.
Reprints and Subscriptions	To order reprints of this article or to subscribe to the journal, contact the AACR Publications Department at pubs@aacr.org.
Permissions	To request permission to re-use all or part of this article, use this link http://clincancerres.aacrjournals.org/content/15/12/4157. Click on "Request Permissions" which will take you to the Copyright Clearance Center's (CCC) Rightslink site.

Downloaded from clincancerres.aacrjournals.org on September 27, 2020. © 2009 American Association for Cancer Research.